https://doi.org/10.20575/00000040
Polar Data Journal, Vol. 6, 32–42, August 2022

Methane flux around the Gulkana Glacier terminus, Alaska summer 2019

Keiko KONYA [1]*, Go IWAHANA [2,3], Tetsuo SUEYOSHI [4], Tomoaki MORISHITA [5], and Takahiro ABE [6]

[1] Japan Agency for Marine-Earth Science and Technology, 3173-25 Showa-machi, Kanazawa-ku, Yokohama, Kanagawa, 236-0001.
[2] International Arctic Research Center, University of Alaska Fairbanks, 2160 Koyukuk Drive, Fairbanks, AK 99775-7340, USA.
[3] Arctic Research Center, Hokkaido University, Kita-21 Nishi-11 Kita-ku, Sapporo, Hokkaido, 001-0021.
[4] National Institute of Polar Research, Research Organization of Information and Systems, 10-3, Midori-cho, Tachikawa, Tokyo, 190-8518.
[5] Forestry and Forest Products Research Institute 92-25 Nabeyashiki, Shimokuriyagawa, Morioka, Iwate, 020-0123.
[6] Graduate School of Bioresources, Mie University, 1577 Kurimamachiya-cho, Tsu, Mie, 514-8507.
*Corresponding author. Keiko Konya (conya@jamstec.go.jp)
(Received September 2, 2021; Accepted June 10, 2022)

Abstract: Methane (CH_4) flux was measured at 18 locations across three sites near the Gulkana Glacier terminus, Alaska Range, in mid-July 2019. These measurements aimed to investigate the CH_4 flux from proglacial land surfaces of temperate mountain glaciers. Flux was measured using a closed chamber technique. At five locations, values of CH_4 flux ranged from 1.8 to 11.0 μg C m^{-2} h^{-1}, whereas no CH_4 flux was detected at the remaining 13 locations. Air and water temperatures, pH, and electric conductivity of puddle and river water were also measured at each location. Stable isotope analysis was conducted on CH_4 and water from puddles and rivers at the observation sites.

1. Background

Methane (CH_4) is the second most important greenhouse gas after carbon dioxide (CO_2), with an estimated global warming potential of 28[1]. The CH_4 concentration in the atmosphere has increased globally since the beginning of the industrial era, and the Arctic region is in general exhibiting higher

concentrations than any other region in the world[2]. The primary sources of CH_4 in the Arctic are wetlands and wet permafrost terrain[3]. Although glaciated areas are not considered to be major sources of CH_4, this view has been questioned in recent studies. A high diffusive CH_4 flux of 4.4–28 mmol of CH_4 m^{-2} d^{-1} has been detected from the runoff at the margin of the Greenland ice sheet, indicating the presence of biologically active wetlands beneath the ice sheet[4]. Subglacial methanogenesis has also been indicated by CH_4 release in meltwater from beneath an Icelandic glacier[5].

As for mountain glaciers, evidence of methanogenesis has also been observed in subglacial sediments in the Canadian Rockies, with a significant level of organic carbon and dissolved CH_4 (16 and 29 ppmv, respectively) being reported in porewater[6]. However, there is still very little data on CH_4 flux from mountain glaciers, which are widely distributed in the high latitudes. Therefore, it is considered that the CH4 flux from Arctic glaciers can be essential for understanding CH4 flux measurements in high latitudes. In this study, we measured the CH_4 flux from the terminus of the Gulkana Glacier, a temperate, small-scale mountain glacier in the Alaska Range. As CH_4 flux can depend on surface and underground conditions, we performed measurements on multiple types of ground surfaces at the front of the glacier terminus. We also measured physical factors, such as temperature and moisture environment. Based on this preliminary case study, we aim to design a more comprehensive study plan to verify the generality of CH_4 emission from the glacier terminus in high latitudes and mountains.

2. Location

The study sites are located near the Gulkana Glacier terminus (63.25 °N, 145.42 °W) in Alaska (Figure 1 a-c). Gulkana Glacier was selected because it is a typical land-terminating and retreating mountain glacier. It is also easy to access, an essential factor for the convenient transportation and deployment of measurement equipment. The Gulkana Glacier is a polythermal glacier 1,160–2,470 m above sea level, with an area of 16.0 km^2 that shrank by 14 % between 1967 and 2016[7]. Sampling was conducted from July 15–16, 2019, one month after the beginning of the glacial melt season.

Measurements were performed at six different locations at three sites, for a total of 18 locations (Figure 1 c-f). The three sites (A, B, and C) were selected for the following reasons: close to the glacier terminus, flat areas allowing for easier deployment of equipment, and surface variability that CH_4 flux depends on. Site A (63.252 °N, 145.431 °W) was farthest, 250 m from the terminus and the side of glacier runoff, suggesting that it was beneath the glacier until recently. This site was chosen to test the hypothesis that subglacial land has a high CH_4 flux. Sites B and C (63.254 °N, 145.427 °W), located closer to the glacier terminus, were 230 and 250 m away from site A. These sites were selected to assess how CH_4 flux varied with distance from the glacier terminus.

3. Methods

We measured CH_4 flux from the ground surfaces using a closed chamber technique[8]. Grounded cylindrical stainless-steel chambers (~20 cm in diameter and 25 cm in height) were inserted 3–5 cm into the ground and left stationary for 5–15 min to reduce internal air disturbance. The heights of the chambers were measured before and after sampling, with an accuracy of 5 mm. Subsequently, 40 mL gas samples were collected using a syringe and injected into 30 mL vacuum glass bottles sealed with butyl rubber stoppers and plastic caps. The samplings were taken 0, 10, 20, and 40 min after the chamber lid was closed. In the laboratory, 2 mL of the gas samples were taken from the rubber stopper of the sample bottle and injected into a gas chromatograph (GC). Samples were analyzed using gas chromatography coupled with a flame ionization detector (FID) at the Forestry and Forest Products Research Institute[9]. The GC-FID (Shimadzu GC-8A, Kyoto, Japan) was equipped with a 2 m Unibeads C column, and its temperature was maintained at 120 °C. We used ultrapure helium gas (99.9999 % pure) as the carrier at a flow rate of 40 mL s^{-1}. The standard gas (1.981 ppmv) (Saisan Co., Ltd) was used for calibration of CH_4 concentration measurement. CH_4 flux was calculated using a temporal gradient of the CH_4 concentration measure by gas chromatography. The CH_4 flux in μg CH_4 C m^{-2} h^{-1} was calculated using the following equation[10]:

$$F = \rho \times V/A \times \triangle c/\triangle t \times 273/T \quad (1)$$

where F is the CH_4 emission rate (flux), ρ is the density of CH_4 under standard conditions (0.716×10^9 μg m^{-3}); V and A are the volume (m^3) and base area (m^2) of the chamber, where V/A means the height of the chamber from the ground surface; $\triangle c/\triangle t$ is the rate of CH_4 concentration change in the chamber during a given period (10^{-6} m^3 m^{-3} h^{-1}) calculated as a slope of linear regression line; and T is the temperature (K).

The stable isotope ratios of carbon ($\delta^{13}C$) of CH_4 were analyzed for gas samples collected 40 min after chamber closure at ten sampling locations. Measurements were made at the University of California Davis Stable Isotope Facility as the 40-min gas samples were expected to have a high CH_4 concentration. The stable isotope ratios of carbon ($\delta^{13}C$) and hydrogen ($\delta^{2}H$) in CH_4 were measured using a Thermo Scientific PreCon concentration unit, interfaced with a ThermoScientific Delta V Plus isotope ratio mass spectrometer (Thermo Scientific, Bremen, Germany). The detection limits for $^{13}C_{CH4}$ and $^{2}H_{CH4}$ measurements were 0.8 and 2 nanomoles (nM), and the standard deviations of the measurements were 0.2‰ and 2 ‰, respectively. Data were expressed relative to the Vienna Pee Dee Belemnite (V-PDB) scale for carbon and the Vienna Standard Mean Ocean Water (V-SMOW) scale for hydrogen.

Stable water isotopes (δD and $\delta^{18}O$) were analyzed from 10-mL water samples from the Gulkana and Maclaren rivers, puddles, and terminal glacier ice. This analysis was done at the Alaska Stable

Isotope Facility, University of Alaska Fairbanks. The δD and $\delta^{18}O$ values were measured using a pyrolysis-elemental analyzer EA-IRMS. This method employed a Thermo Scientific high-temperature element analyzer (TC/EA) and a Conflo III interface with a Delta XP isotope ratio mass spectrometer. Stable isotope ratios were reported in δ notation as parts per thousand (‰) deviations V-SMOW. The instrument precision was smaller than 1.2‰ and 0.2 ‰ for δD and $\delta^{18}O$ measurements, respectively. Measurements of air and water temperature were made on-site using a D717 portable temperature sensor (Techno Seven, Tokyo, Japan) Electrical conductivity and pH were also measured on-site using B-771 and B-712 mobile sensors (HORIBA, Kyoto, Japan), respectively.

4. Data Records

Table 1 shows the values of CH_4 concentration in gas samples after 0, 10, 20, and 40 min and the calculated values of CH_4 flux at all 18 locations (methane_concentration_2019.csv). Values of CH_4 flux, $\delta^{13}C$, electrical conductivity, air and water temperature, and CH_4 concentration are shown in Table 2 (flux_data_2019.csv). Table 3 shows the δD and $\delta^{18}O$ isotope ratios of the ice and water samples (isotope_data2019.csv). Figure 2 and Table 1 show a positive CH_4 flux at five of the 18 locations; two at site A, two at site B, and one at site C. The surface types of all five of these locations were either puddles or sand (Table 2). Location data (latitude and longitude) can be found in locations_flux_2019.csv.

5. Technical Validation

Gas chromatography measurements were obtained with a precision of 0.01 ppmv. Consequently, temporal changes in CH_4 concentrations less than 0.01 ppmv were considered to be undetected, and these values are shown as 0 in Table 1. Regarding the accuracy of the flux calculations, exceptional treatments are required for locations with minimal fluxes. Unlike the case of general flux observations, we need to evaluate if the significant CH_4 fluxes are lacking for these locations. Firstly, the flux is considered to be 0 when the CH_4 concentration change is too small ($\triangle c < 0.01$). Secondly, the squared correlation coefficient between the CH_4 concentration and the time from the start of observation was calculated. This analysis was conducted to test the linearity of the time series of CH_4 concentrations. Then, the calculated values were rejected when the squared correlation coefficient was very low ($R^2 < 0.6$). By this criterion, CH_4 fluxes at A6 and B6 were not considered to be detectable, and the flux was not calculated from concentrations. The error for significant flux calculations is listed in the flux column in Table 2 and shown as the error bar in Figure 2. As flux values are calculated from the slope of $\triangle c/\triangle t$ using equation (1), the determining accuracy of the slope ($\triangle c/\triangle t$) gives the accuracy of the flux. The error of flux was derived from the standard error of determining the slope of $\triangle c/\triangle t$, i.e., the

standard error of the regression line for the four data points. We did not evaluate the error caused by in-situ observations, which is difficult to quantify.

Electrical conductivity was measured to an accuracy of ±0.6% of full scale. The resolution and accuracy of air temperatures were 0.1 and ±0.4 °C, respectively, and the accuracy of the pH sensor was 0.01.

6. Figures

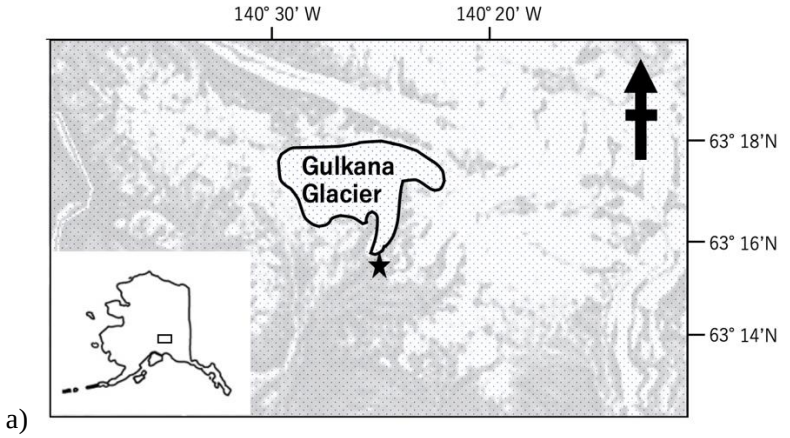

a)

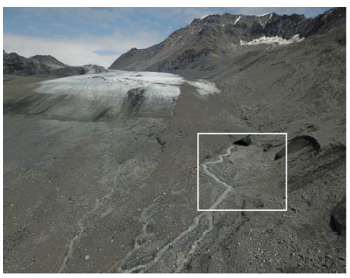

b)

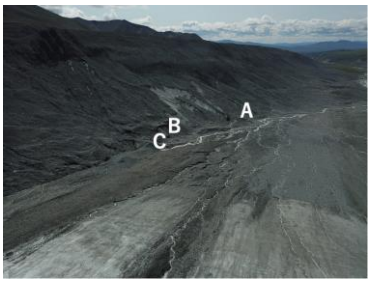

c)

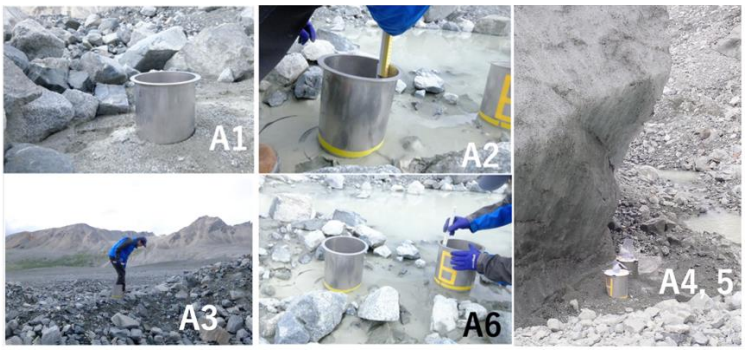

d)

e)

f)

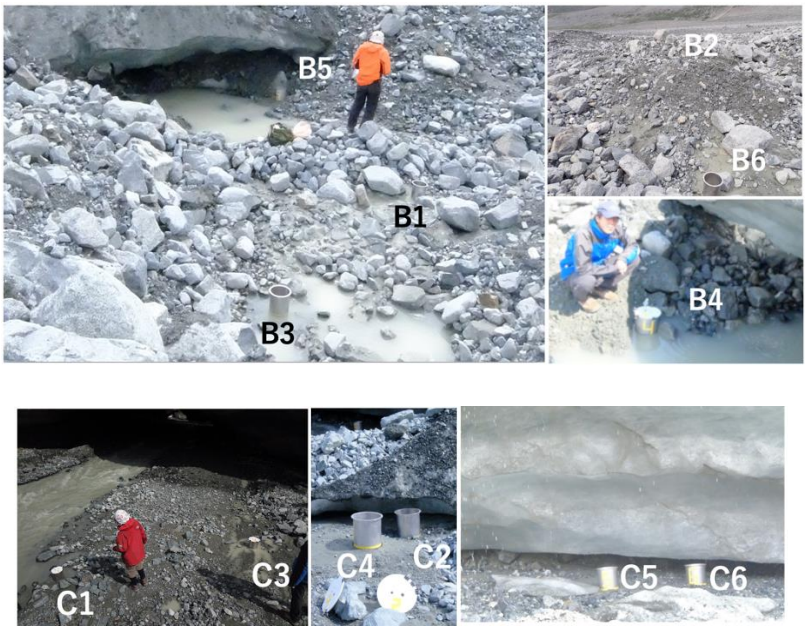

Figure 1. a) A map of the sampling site at the terminus of the glacier. The solid black line indicates the location of the Gulkana Glacier. The background is a satellite image, with glaciers and rivers shown as white areas. The star shows the sampling site. b) An aerial photograph of the Gulkana Glacier looking upstream towards the glacier. The white box outlines the study area. c) A photograph of the study area looking downstream from the glacier, showing the locations of the three test sites A, B, and C, indicated in the panels d), e), and f). d) The six sampling locations at site A. The surface conditions are shown in Table 2. A4 and A5 are besides large ice mass. The metal cylinders shown in panels d), e), and f) are flux chambers. e) The six sampling locations at site B. B5 is located at the entrance to a small ice tunnel. f) The six sampling locations at site C. C1 are in the puddle in which glacier discharge water comes.

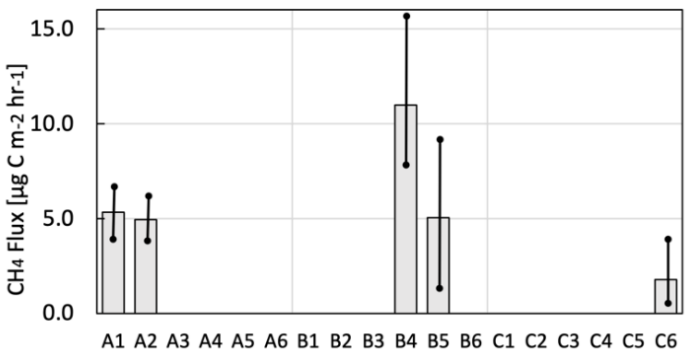

Figure 2. CH_4 fluxes at all 18 locations. The error bar shows the estimated standard error shown in Table 2. Only five locations (A1, A2, B4, B5, and C6) had a measurable CH_4 flux. The sample locations are indicated by the labels along the bottom of the chart.

7. Tables

Table 1. CH_4 concentrations (ppmv) at sampling time, chambers height, and calculated CH_4 flux for 18 locations. "–" denotes failure in the collection of the gas sample from the bottle to the tube connecting the sensor in the gas chromatography devise. A sample was taken for each sampling time (0, 10, 20, and 40 min after the chamber lid was closed). Flux is considered to be 0 when the CH_4 concentration change is too small ($\triangle c < 0.01$). $\triangle c$ denotes CH_4 concentration change in a certain time. Flux calculation was also rejected when the squared correlation coefficient between the concentration value and the linear regression line to estimate $\triangle c/\triangle t$ was very low (<0.6). These results were rejected as they were considered to be inaccurate. The chamber heights were 19–24 cm, measured at 5 mm intervals, and averaged.

Location	CH_4 concentration at each sampling time				Chamber height [m]	CH_4 Flux [μg CH_4 C m^{-2} h^{-1}]
	0 min	10 min	20 min	40 min		
A1	1.858	1.876	–	1.897	0.190	5.3
A2	1.887	1.900	1.906	1.917	0.226	4.9
A3	1.915	1.902	1.900	–	0.239	0 ($\triangle c < 0.01$)
A4	1.894	1.909	1.897	1.889	0.206	0 ($\triangle c < 0.01$)
A5	1.887	1.897	1.890	1.892	0.216	0 ($\triangle c < 0.01$)
A6	1.900	1.870	1.888	1.913	0.229	0 ($R^2 < 0.6$)
B1	1.915	1.914	1.914	1.924	0.214	0 ($\triangle c < 0.01$)
B2	1.936	–	1.938	1.921	0.206	0 ($\triangle c < 0.01$)
B3	1.911	1.897	1.901	1.905	0.208	0 ($\triangle c < 0.01$)
B4	1.901	1.903	1.900	1.981	0.171	11.0
B5	1.902	1.933	–	1.938	0.223	5.1
B6	1.952	1.937	1.991	1.931	0.188	0 ($R^2 < 0.6$)
C1	1.900	–	1.914	1.911	0.205	1.8
C2	1.891	1.920	1.917	1.904	0.218	0 ($\triangle c < 0.01$)
C3	–	1.915	1.909	1.904	0.201	0 ($\triangle c < 0.01$)
C4	1.902	n/d	1.904	1.895	0.206	0 ($\triangle c < 0.01$)
C5	1.908	1.917	1.915	1.907	0.198	0 ($\triangle c < 0.01$)
C6	1.915	1.922	1.921	1.928	0.219	0 ($\triangle c < 0.01$)

Table 2. Sample locations and measured parameters. Sample number to estimate CH_4 flux was 3 or 4 for each location as shown in Table 1. n/m indicates that no measurement data was available. Ta and Tw represent that temperature measurements are the air and puddle water temperatures, respectively. * indicates that pH was measured at the puddles or river next to the flux observation chambers. S and W indicate whether the surface was sand (S) or water (W), respectively.

Location	CH_4 Flux [μg C m^{-2} h^{-1}]	$\delta^{13}C_{CH4}$ [‰] (CH_4 concentration for $\delta^{13}C_{CH4}$ [ppm])	Electrical conductivity [mS/cm]	Air/water temperature [ºC]	pH	Ground-surface conditions	Date and time
A1	5.3 ± 1.2	n/m	n/m	n/m	n/m	S (wet)	July 15, 15:20–17:50
A2	4.9 ± 0.8	n/m	n/m	n/m	n/m	S (wet)	
A3	0	n/m	n/m	n/m	n/m	S (dry)	
A4	0	n/m	n/m	14.4 (Ta)	n/m	S (wet)	
A5	0	-44.77 (1.52)	0.111	3.1 (Tw)	8.4*	S (wet)	
A6	0	-44.46 (1.50)	0.152	5.8 (Tw)	n/m	S (wet)	
B1	0	-44.90 (1.51)	n/m	6.5 (Ta)	8.57	S (wet)	July 16, 12:15–13:50
B2	0	-44.63 (1.54)	n/m	n/m	8.74	S (dry)	
B3	0	-44.61 (1.54)	0.124	3.8 (Tw)	n/m	W (puddle)	
B4	11.0 ± 4.3	-44.57 (1.53)	0.127	6.5 (Ta) 2.0 (Tw)	n/m	W (puddle)	
B5	5.1± 4.1	-44.42 (1.51)	n/m	n/m	n/m	S (wet)	
B6	0	-44.80 (1.52)	n/m	n/m	n/m	S (dry)	
C1	1.8 ± 1.6	-44.84 (1.57)	n/m	8.4 (Ta) 0.7 (Tw)	8.18*	W (puddle)	July 16, 14:14–15:50
C2	0	-44.93 (1.49)	0.071	n/w	n/m	S (wet)	
C3	0	-44.81 (1.56)	n/m	n/m	n/m	W (Puddle)	
C4	0	-46.28 (1.87)	n/m	n/m	n/m	S (wet)	
C5	0	-44.76 (1.55)	n/m	n/m	n/m	S (wet)	
C6	0	-44.79 (1.63)	n/m	n/m	n/m	S (wet)	

Table 3. Hydrogen and oxygen stable isotope ratios for water and ice at sites A, B, and C. Melted ice was collected from debris-covered ice near the sampling sites. Water samples from the Maclaren River were collected at the riverside next to the lodge (63.119071 °N, 146.531962 °W). The "stdev" denotes the standard deviation.

Sampling location	δD [‰ VSMOW]	δD (stdev) [‰ VSMOW]	$\delta^{18}O$ [‰ VSMOW]	$\delta^{18}O$ (stdev) [‰ VSMOW]
A5_melted ice (1)	-166.23	1.87	-23.15	0.33
A5_melted ice (2)	-148.34	0.34	-21.06	0.08
A6_puddle (1)	-163.54	2.24	-23.53	0.39
A6_puddle (2)	-153.68	0.35	-23.30	0.10
B3_puddle	-161.06	0.55	-22.20	0.08
B4_puddle	-161.20	1.00	-22.37	0.41
B5_melted ice (1)	-157.17	0.33	-22.03	0.36
B5_melted ice (2)	-169.41	0.51	-22.77	0.28
C1_glacier discharge	-166.65	0.41	-20.37	0.40
C6_melted ice (1)	-167.12	0.55	-22.57	0.39
C6_melted ice (2)	-158.18	0.72	-21.73	0.27
Maclaren river water (1)	-164.89	0.81	-22.37	0.12
Maclaren river water (2)	-164.54	0.90	-22.50	0.22

Author contributions

Konya K. conducted the field measurements and drafted the manuscript. Iwahana G. arranged the field logistics and conducted fieldwork. Sueyoshi T. led this project. Morishita T. prepared the CH_4 flux measurement system and analyzed CH_4 concentrations. Abe T. conducted field measurements. All authors contributed to the revision of the manuscript.

Acknowledgments

This study was partially supported by the Grant for Joint Research Program of the Japan Arctic Research Network Center. This work was part of the Arctic Challenge for Sustainability II (ArCS II), Program Grant Number JPMXD1420318865.

References

1. Stocker, T. F., Qin, D., Plattner, G.-K., Tignor, M. M. B, Allen, S.K., Boschung, J., Nauels, A., Xia, Y., Bex, V. and Midgley, P. M. (eds.) IPCC. Climate Change 2013: The Physical Science Basis. Contribution of Working Group I to the Fifth Assessment Report of the Intergovernmental Panel on Climate Change. Cambridge University Press, Cambridge, United Kingdom and New York, USA. 2013, 1535 p.
2. Japan Meteorological Agency. Greenhouse gases, Methane (CH_4). https://www.data.jma.go.jp/ghg/kanshi/ghgp/ch4_e.html (accessed year-month-date).
3. Taylor, M. A., Celis, G., Ledman, J. D., Bracho, R. and Schuur, E. A. G. Methane Efflux Measured by Eddy Covariance in Alaskan Upland Tundra Undergoing Permafrost Degradation. J. Geophys. Res. Biogeosciences. 2018, 123, p. 2695–2710. https://doi.org/10.1029/2018JG004444.
4. Lamarche-Gagnon, G., Wadham, J. L., Lollar, B. S., Arndt, S., Fietzek, P., Beaton, A. D., Tedstone, A. J., Telling, J., Bagshaw, E. A., Hawkings, J. R., Kohler, T. J., Zarsky, J. D., Mowlem, M. C., Anesio, A. M. and Stibal, M. Greenland melt drives continuous export of methane from the ice-sheet bed. Nature. 2019, 565, p. 73–77. https://doi.org/10.1038/s41586-018-0800-0.
5. Burns, R., Wynn, P. M., Barker, P., McNamara, N., Oakley, S., Ostle, N., Stott, A. W., Tuffen, H., Zhou, Z., Tweed, F. S., Chesler, A. and Stuart, M. Direct isotopic evidence of biogenic methane production and efflux from beneath a temperate glacier. Scientific Reports. 2018, 8, 17118. https://doi.org/10.1038/s41598-018-35253-2.
6. Boyd, E. S., Skidmore, M., Mitchell, A. C., Bakermans, C. and Peters, J. W. Methanogenesis in subglacial sediments. Environmental Microbiology Reports. 2010, 2, p. 685–692. https://doi.org/10.1111/j.1758-2229.2010.00162.x.
7. O'Neel, S., McNeil, C., Sass, L. C., Florentine, C., Baker, E. H., Peitzch, E., McGrath, D., Fountain, A. G. & Fagre, D. Reanalysis of the US Geological Survey Benchmark Glaciers: long-term insight into climate forcing of glacier mass balance. Journal of Glaciology. 2019, 65, p. 850–866. https://doi.org/10.1017/jog.2019.66.
8. Morishita, T., Noguchi, K., Kim, Y. and Matsuura, Y. CO_2, CH_4 and N_2O fluxes of upland black spruce (*Picea mariana*) forest soils after forest fires of different intensity in interior Alaska. Soil Science and Plant Nutrition. 2015, 61, p. 98–105. https://doi.org/10.1080/00380768.2014.963666.
9. Morishita, T., Sakata, T., Takahashi, M., Ishizuka, S., Mizoguchi, T., Inagaki, Y., Terazawa, K., Sawata, S., Igarashi, M., Yasuda, H, Koyama, Y., Suzuki, Y., Toyota, N., Muro, M., Kinjo, M., Yamamoto, H., Ashiya, D., Kanazawa, Y., Hashimoto, T. and Umata, H. Methane uptake and nitrous

oxide emission in Japanese forest soils and their relationship to soil and vegetation types. Soil Science and Plant Nutrition. 2007, 53, p. 678–691. https://doi.org/10.1111/j.1747-0765.2007.00181.x.

10. Morishita, T., Hatano, R., Nagata, O., Sakai, K., Koide, T. and Nakahara, O. Effect of nitrogen deposition on CH^4 uptake in forest soils in Hokkaido, Japan. Soil Science and Plant Nutrition. 2004, 50 (8), p. 1187–1194. https://doi.org/10.1080/00380768.2004.10408593.

Data Citation

Konya, K., Iwahana, G., Morishita, T. Sueyoshi, T. and Abe T. Methane flux observation at Gulkana Glacier terminus, Alaska in July 2019. 1.10, Japan, Arctic Data archive System (ADS), 2021. https://doi.org/10.17592/001.2021072001.